POLITECNICO DI TORINO
Repository ISTITUZIONALE

Net heat-flux measurement method for passive radiative cooling materials with ambient self-tracking

Original
Net heat-flux measurement method for passive radiative cooling materials with ambient self-tracking / Bertiglia, F., Forte, D., Lopardo, G., Girard, F., Fasano, M., Pattelli, L.. - In: APPLIED THERMAL ENGINEERING. - ISSN 1359-4311. - ELETTRONICO. - 303:(2026). [10.1016/j.applthermaleng.2026.132228]

Availability:
This version is available at: 11583/3012908 since: 2026-07-10T07:44:30Z

Publisher:
Elsevier

Published
DOI:10.1016/j.applthermaleng.2026.132228

Terms of use:

This article is made available under terms and conditions as specified in the corresponding bibliographic description in the repository

Publisher copyright

(Article begins on next page)

08 November 2026

Applied Thermal Engineering 303 (2026) 132228

Contents lists available at ScienceDirect

Applied Thermal Engineering

journal homepage: www.elsevier.com/locate/ate

Research Paper

Net heat-flux measurement method for passive radiative cooling materials with ambient self-tracking

Fabio Bertiglia [a], Davide Forte [b], Giuseppina Lopardo [a], Ferruccio Girard [a], Matteo Fasano [b], Lorenzo Pattelli [a,*]

[a] Istituto Nazionale di Ricerca Metrologica, Strada delle Cacce 91, Torino, 10135, Italy
[b] Department of Energy, Politecnico di Torino, Corso Duca degli Abruzzi 24, Torino, 10129, Italy

ARTICLE INFO

Dataset link: https://doi.org/10.5281/zenodo.18310769, https://github.com/davideforte99/Net-Heat-Flux-of-Radiative-Cooling-Materials

Keywords:
Passive radiative cooling
Net cooling power
Net heat flux density
Radiative heat transfer
Ambient tracking
Metrology

ABSTRACT

Passive Radiative Cooling (PRC) materials can efficiently dissipate thermal energy to outer space through the atmospheric window (8–14 μm), while reflecting most incident solar radiation, enabling sub-ambient cooling under direct sunlight. This work presents RAFT (Radiative Ambient-referenced Flux Testbed), a compact device for accurate outdoor PRC materials characterization. RAFT employs a heat flux meter to directly measure net heat flux, with the PRC sample mounted on the sensing surface and thermally coupled to an ambient-tracked reservoir via a compact fan-based convective heat exchanger integrated with heat pipes. Outdoor experiments demonstrated reliable ambient temperature tracking and accurate net heat flux measurements, which were further verified using an openly-released numerical model. Compared with conventional resistive heater-based outdoor setups, RAFT overcomes key limitations: it eliminates the need for feedback-control, shortens the measurement chain, reduces measurement noise when sample temperature approaches ambient, and enables quantification of both cooling and heating net fluxes with a total measurement uncertainty of $\pm 1.8\,\mathrm{W\,m^{-2}}$. Relative to liquid-flow-based systems, RAFT offers improved portability and avoids the complexities of fluid handling. The proposed setup provides a robust and practical framework for outdoor evaluation of PRC materials, addressing the current lack of standardized protocols for direct heat flux measurement.

1. Introduction

The intensification of climate change presents a growing threat to worldwide energy security [1]. Rising global temperatures are driving a rapid increase in demand for space cooling, which is projected to more than double by 2040 [2]. In this context, the development of sustainable and energy-efficient cooling materials is critical, and passive radiative cooling (PRC) technologies have emerged as a promising solution [3–5]. PRC materials are capable of efficiently dissipating thermal radiation through the atmospheric window (8–14 μm), a spectral region in which the Earth's atmosphere exhibits high transparency. Through this mechanism, thermal energy is directly dissipated to outer space, which acts as an infinite cold sink [6]. When the optical properties of PRC materials are tuned to also exhibit high reflectivity across the solar spectrum (0.3–2.5 μm), daytime radiative cooling can be achieved, enabling the material to maintain a sub-ambient temperature even under direct solar irradiance [7].

Although a large variety of materials exhibiting daytime radiative cooling properties has been proposed in the literature [8], there are no established methodologies, configurations or boundary conditions to assess their individual performance [9]. This lack of consistency highlights the need for more accessible experimental testing protocols and standardized figures of merit.

Because PRC performance depends on highly variable environmental conditions, several studies have explored indoor experimental platforms aimed at improving repeatability and controllability of testing conditions [10–16]. Nonetheless, outdoor testing remains uniquely relevant since the radiative cooling effect is inherently coupled to the real sky dome and its time- and location-dependent state. In particular, the downwelling longwave radiance depends not only on the atmospheric transmission spectrum (e.g., the water vapor column) but also on cloud cover, aerosols, and the angular distribution of sky emission, which are difficult to reproduce in a test chamber [14,17]. Field performance is also uniquely affected by wind and buoyancy-driven convection, transient solar conditions, and practical deployment factors such as view factor to the sky. As a result, laboratory-based protocols can be useful as complementary tools, whereas outdoor measurements remain the only reference for assessing PRC materials under realistic operating conditions.

* Corresponding author.
E-mail address: l.pattelli@inrim.it (L. Pattelli).

https://doi.org/10.1016/j.applthermaleng.2026.132228
Received 11 March 2026; Received in revised form 28 June 2026; Accepted 2 July 2026
Available online 8 July 2026
1359-4311/© 2026 The Authors. Published by Elsevier Ltd. This is an open access article under the CC BY license (http://creativecommons.org/licenses/by/4.0/).

Outdoor experiments therefore play a central role in PRC validation, despite the relevant volatility of environmental variables which often require the realization of complex setups and shielding conditions. Accordingly, recent work has emphasized best-practice guidelines for outdoor PRC testing, including apparatus geometry, sensor placement, view-factor control, and the standardized acquisition of atmospheric context data [9,18–20]. From a practical standpoint, the field experiments need outdoor setups that are not only accurate, but also portable, repeatable, and accessible to non-specialist users.

In this context, two figures of merit are commonly reported for PRC materials characterization: the stagnation temperature and the net cooling flux at thermal equilibrium with the ambient environment [20]. The former quantifies the lowest temperature reached by the sample under a given set of outdoor boundary conditions and occurs when the net heat flux vanishes ($q_{net} = 0$). While apparently simple to measure, stagnation temperature is not an intrinsic property of the coating alone: it also depends on the thermal mass and non-radiative heat exchange characteristics of the supporting substrate. Lightweight or weakly coupled substrates can exhibit large sub-ambient temperature drops even when the actual net cooling power of the coating is limited, making stagnation temperature a configuration-dependent metric that may not represent performance under realistic operating conditions.

For practical applications, a more relevant metric is therefore represented by the net cooling flux ($W\,m^{-2}$) evaluated near thermal equilibrium with the ambient environment, defined as the net flux when the sample temperature (T_s) equals the ambient temperature (T_{amb}). By operating near T_{amb}, this metric directly quantifies how much heat a PRC surface can remove from an attached load under realistic boundary conditions, while reducing sensitivity to temperature-driven parasitic heat exchange pathways that can strongly bias sub-ambient stagnation measurements.

Most outdoor experimental setups estimate this quantity indirectly from electrical heating measurements [7,21–23]. In these configurations, a resistive heater beneath the sample is actively controlled to maintain $T_s \approx T_{amb}$, and the required Joule power is interpreted as the net cooling power. Besides requiring a power supply and feedback controller, this approach introduces an extended measurement chain (electrical power plus multiple temperature measurements), so uncertainty propagation and parasitic heat exchange pathways (e.g., lateral conduction or imperfect guarding) can bias the inferred flux.

Use of heat-flux sensors, which often incorporate built-in lateral thermal guarding, remains sporadic and typically integrated within actively driven heater-based measurement chain [24], rather than enabling a passively ambient-referenced net-flux measurement architecture. Additionally, all heater-based implementations inherently cannot report net *heating* conditions: when the radiative surface tends to warm above ambient, the heater simply turns off and the inferred "cooling power" clamps to zero rather than changing sign.

An alternative approach uses calorimetric rigs in which a heat-transfer liquid flows beneath the PRC sample [25–28]. In this case, the net cooling flux is inferred from the measured liquid temperature rise/drop across the device, the mass flow rate, and the liquid specific heat capacity, normalized by the sample area. While robust in many contexts, calorimetric measurements inherently require a finite temperature gradient in the working fluid and typically rely on multiple sensors (inlet/outlet temperatures and flow rate), so the uncertainty can be dominated by differential measurements and by variable heat exchanges to the environment along the temperature gradient.

A practical limitation shared by heater-based and calorimetric approaches is the reliance on differential temperature measurements obtained from independent sensors at distinct locations (e.g., T_s vs. T_{amb}, or inlet vs. outlet temperatures). Given typical temperature sensor uncertainties, this can quickly compound to several $W\,m^{-2}$ of uncertainty in inferred cooling power under outdoor convection conditions, even without considering additional contributions from electric resistance and current uncertainties, or liquid flow rate uncertainties.

This work introduces an alternative outdoor method to measure the ambient-referenced net cooling flux of PRC materials, designed to be simple, accessible, and with low uncertainty. The device proposed, hereafter referred to as RAFT (Radiative Ambient-referenced Flux Testbed), is a compact and portable platform using a heat-flux sensor between the PRC emitter and a convective heat exchanger, enabling passive ambient-temperature tracking (by natural or low-power forced convection) without an active thermal feedback controller. Unlike resistive-heater or liquid-flow approaches, RAFT relies on a direct measurement of net heat flux, minimizing uncertainty propagation from multiple auxiliary measurements and enabling seamless capture of both cooling and heating regimes. Furthermore, by lifting the need for an actively controlled feedback loop logic, RAFT ensures stable operation near ambient conditions while maintaining high portability, thereby overcoming key limitations of other state-of-the-art devices for outdoor heat-flux measurements of PRC materials.

The remainder of the manuscript is organized as follows. Section 2 describes RAFT in detail, including its design, uncertainty analysis, outdoor testing procedures, and numerical modeling. Section 3 presents the experimental results and model validation, while Section 4 concludes with key findings, limitations, and future directions.

By overcoming key drawbacks of resistive heater- and flowing fluid-based setups, RAFT provides a practical and reproducible approach for measuring radiative cooling performance and has the potential to become a widely adopted, low-uncertainty method for the outdoor evaluation of PRC materials.

2. Methods

2.1. Experimental setup

The RAFT device, shown in Fig. 1a–b, consists of (i) heat-flux and temperature sensors (whose characteristics are summarized in Table S1), (ii) a fan-cooled heat sink, (iii) the PRC sample under test, and (iv) a structural frame supporting all components. For outdoor operation, RAFT is enclosed within a protective casing (Fig. 1b1) designed to shield the device, enhance thermal insulation, and provide shading to the heat sink to ensure stable performance.

The heat flow meter (model HFP01, Hukseflux) is a thermopile-based sensor with a ceramic-plastic body (80 mm diameter, 5.4 mm thickness, thermal conductivity $0.76\,W\,m^{-1}\,K^{-1}$) and a circular sensing area of 32 mm diameter surrounded by a thermal guarding ring. Its measurement range spans from $-2000\,W\,m^{-2}$ to $2000\,W\,m^{-2}$, fully compatible with the net heat fluxes associated with PRC materials, whose thermodynamic limit is approximately $160\,W\,m^{-2}$ [4]. The sensor operates passively and does not require external power. The HFP01 measures the temperature difference across its body using an embedded thermopile. Owing to the low thermal resistance of the sensor body ($R_{th} = 71 \times 10^{-4}\,K\,m^2\,W^{-1}$), the temperature drop across the sensor remains sub-kelvin over the flux range relevant to PRC, keeping the emitter side close to the ambient-referenced heat exchanger.

The temperature of the system is measured by a Pt100 (manufacturer RS PRO) resistance temperature detector (RTD) positioned within a small cavity drilled into the aluminum plate. Thermal contact between the Pt100 element and the aluminum plate is ensured by a thermally conductive paste (RS PRO silicone thermal grease, $3.9\,W\,m^{-1}\,K^{-1}$), and the sensor is held in place using aluminum tape. The conductive aluminum plate (100 mm×100 mm×2.5 mm) provides the thermal interface between the heat-flow meter and the fan-cooled heat sink. The Pt100 sensor is used to monitor the temperature of the convective heat exchanger assembly (hereafter T_{ref}), which serves purely a diagnostics role and supports model validation. Importantly, T_{ref} is not used to infer the heat flux: the primary measurement of net heat exchange is obtained directly from the HFP01 output, independent of ambient or sample temperature measurement.

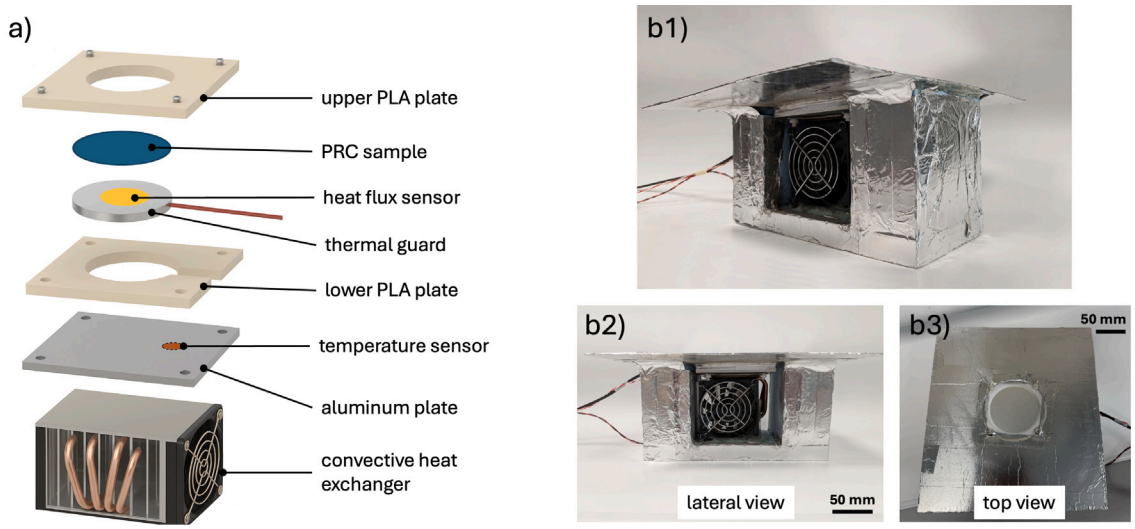

Fig. 1. (a) Exploded-view schematic of the RAFT apparatus. (b1) Photograph of the RAFT apparatus with its external casing; (b2) lateral view; (b3) top view.

The outputs from the flux meter and temperature sensor are acquired by a $6^1/_2$-digit digital multimeter/data-acquisition system (model 2700, Keithley). The instrument records the thermopile voltage of the heat-flux sensor together with the four-wire resistance measurement of the Pt100 sensor, time-stamps the data, and stores them in the internal buffer of the data-acquisition unit. The data stream is then transferred to a laptop running a LabVIEW interface, where the measurements are displayed in real time and logged for subsequent analysis. The heat flux and temperature signals are acquired at a 30 s sampling interval.

The fan-cooled heat sink (90 mm×90 mm×90 mm) is a standard module commonly employed for central processing unit (CPU) cooling in personal computers. The unit incorporates a compact fan (12-volt supply voltage) and 3 copper heat pipes to enhance heat dissipation. According to the manufacturer's specifications, the heat sink can dissipate a maximum heat flux of 150 W, which is sufficient to ensure rapid ambient-temperature tracking. The fan operates in suction mode, extracting air from within the device; this configuration is more effective than blowing mode as it prevents the minor heating of the airflow that occurs when air is forced through the fan blades. The fan airflow remains confined within the heat exchanger assembly and does not directly interact with the PRC sample surface.

To test the device, we applied a commercial PRC material sample supplied as a thin film with an adhesive backing. The sample was cut into a circular shape with a diameter of 8 cm and adhered directly onto the heat-flow meter.

The heat flux meter is held in place between two insulating plates (100 mm×100 mm×2.5 mm), each featuring a central circular aperture matching the heat-flow meter dimensions. The two plates are made of polylactide (PLA) and fabricated via fused-deposition modeling using a 3D printer (model Ender-6, Creality); they are fastened together using four nylon bolts.

To ensure effective ambient-temperature tracking, it is essential to suppress any additional heat gain transferred to the heat sink from the surrounding environment. For this purpose, during the experimental campaign, the RAFT apparatus was enclosed within a casing designed to minimize both radiative and conductive heat gains from the environment. Two expanded polystyrene (EPS) panels (thermal conductivity 0.035 $W\,m^{-1}\,K^{-1}$, thickness 60 mm) were positioned on the two lateral sides of the device not affected by the forced airflow through the heat sink (Fig. 1b2). An additional EPS layer (20 mm) was placed on the bottom surface. On the top surface (Fig. 1b3), a polymethyl methacrylate (PMMA) panel (300 mm×250 mm×1 mm) was installed to provide shading for the heat sink; an aperture was included to allow unobstructed exposure of the PRC sample to the sky. All external surfaces were coated with aluminum tape (manufacturer Tesa), in order to reduce the absorbed solar radiation.

2.2. Outdoor measurements

To evaluate the outdoor performance of the PRC sample, the RAFT setup was installed on the roof platform (Fig. 2a) of a building at the Italian National Institute of Metrological Research (INRiM) in Turin (45°0′58″ N, 7°38′22″ E), Italy. The apparatus was mounted in horizontal position on a parapet at a height of 1.5 m above the roof surface to minimize the influence of thermal radiation emitted by the ground while maximizing exposure to the sky. As shown in the fisheye image in Fig. 2b1, the PRC sample exhibited excellent sky exposure, with a sky view factor (SVF) estimated at 94 % [29] (Fig. 2b2).

Accurate measurement of outdoor conditions is essential for the characterization of PRC materials, as their cooling performance is strongly influenced by atmospheric parameters, primarily air temperature, relative humidity, and cloud cover [17,30]. For this reason, a weather station (model MAXIMET GMX501, Gill Instruments Ltd) was installed near the RAFT setup and at the same height (Fig. 2a), monitoring air temperature (T_{amb}), relative humidity (RH), solar irradiance (G), and wind speed (v). These atmospheric measurements are used to document boundary conditions and to parameterize the theoretical model; they do not contribute to the experimental determination of the instantaneous heat flux.

An infrared temperature sensor (model CS LT, Optris), operating in the spectral range 8–14 μm, was also included in the outdoor measurement configuration. The sensor, positioned near both the weather station and the RAFT setup (Fig. 2a), was oriented toward the sky to measure the infrared sky temperature (T_{sky}). It operates over a wide temperature range (−50 °C to 1030 °C) and provides a qualitative indication of the apparent sky temperature in the spectral range 8–14 μm, enabling the detection of transient variations in cloud cover, haze or aerosol that can induce abrupt variations in the net cooling flux of PRC materials.

Data from the weather station and the infrared temperature sensor were directly acquired by a laptop and stored locally. The characteristics and uncertainties of all sensors used in this study are reported in the Supplementary Material (Table S1).

The RAFT setup can be used to test any type of PRC material, provided that it is directly applied onto the heat-flow meter. During the outdoor performance test, we adopted a commercial PRC sample made of a polymer emitter onto a silver reflector, whose emissivity spectrum, characterized by the Physikalisch-Technische Bundesanstalt using their reference Emissivity Measurements in Air Facility [31], is shown in Fig. 2c. The coating exhibits a weighted average solar reflectivity (0.25–2.5 μm) of 90.5 % and an infrared emissivity within the atmospheric window of 91.4 %.

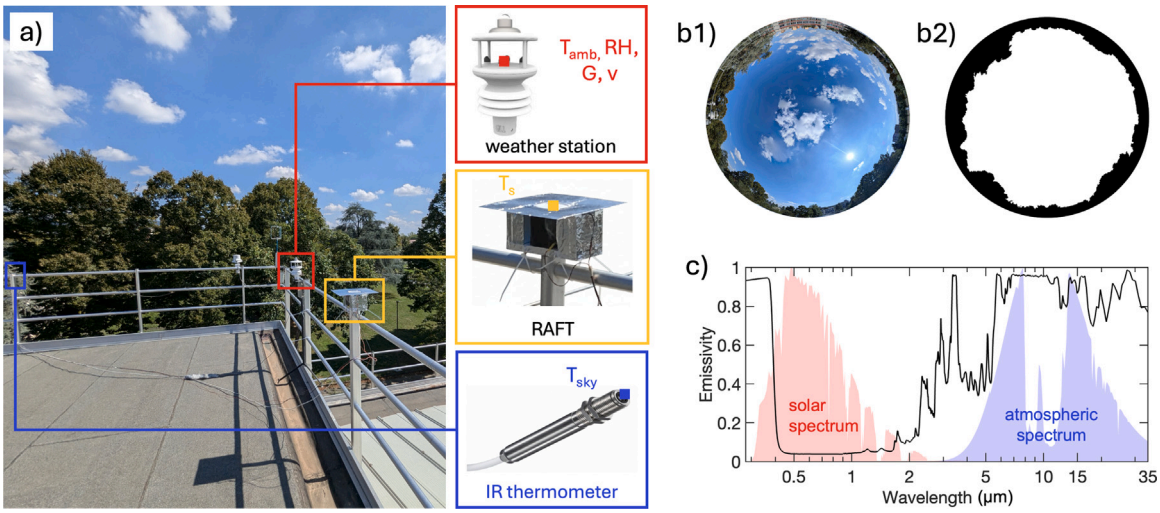

Fig. 2. (a) Photograph of the outdoor measurement setup, including RAFT, the weather station, and the infrared thermometer. (b1) Fisheye image of the sky view as seen from the setup position. (b2) Post-processed fisheye image highlighting obstructions (black) and sky region (white). (c) Spectral emissivity in the 0.25–35 μm range for the commercial PRC sample considered for this test.

Table 1
Uncertainty budget for heat flux measurement.

Source of uncertainty	Value	Probability Distribution	Sensitivity coefficient	Std. uncertainty ($W m^{-2}$)
Digital multimeter	1 mV	normal ($k = 1$)	$0.0295\ W m^{-2} mV^{-1}$	0.030
Heat flux meter uncertainty	$60\ W m^{-2}$	normal ($k = 1$)	3 %	0.900
Temperature dependence effect	25 °C	normal ($k = 1$)	$0.10\ (W/m^2)\%/°C$	0.013
Combined uncertainty (k=2)				**1.8**

2.3. Uncertainty analysis

The overall uncertainty budget of the RAFT system was evaluated, yielding a combined expanded uncertainty of $\pm 1.8\ W m^{-2}$ ($k = 2$) for the measured heat flux. The dominant contribution arises from the intrinsic calibration uncertainty of the heat-flux sensor (~3 %), while contributions from the data acquisition system and temperature dependence remain secondary. The temperature dependence term was conservatively evaluated at a fixed reference temperature of 25 °C, as its variation over the range of ambient temperatures encountered during the measurements is negligible. Table 1 reports the results of the uncertainty analysis for the heat flux measurement, together with the assumptions adopted for the calculation.

Remarkably, this uncertainty is comparable to, or lower than, that obtained by significantly more complex state-of-the-art calorimetric setups once realistic natural-convection conditions are accounted for [28]. This uncertainty reduction is achieved by directly measuring the heat flux, thereby avoiding differential temperature measurements obtained from sensors at distinct locations. The limited thickness of the sensor further reduces sensitivity to parasitic heat transfer pathways, such as lateral conduction. It also removes the need for accurate determination of the sample area and avoids the degradation of the signal-to-noise ratio typical of temperature-difference-based methods near ambient conditions.

2.4. Theoretical model

A numerical model was developed to validate the measurements obtained with the RAFT setup. Implemented in MATLAB, the model is openly accessible online and can serve two primary purposes: (i) to estimate the net cooling power of a generic PRC surface based on its temperature and meteorological conditions, and (ii) to validate net heat flux measurement setups analogous to RAFT.

By applying the first principle of thermodynamics to a PRC surface facing the sky under steady-state conditions, the net cooling flux (q_{net}) is expressed as:

$$q_{net} = q_{rad} - q_{sol} - q_{atm} - q_{obs} - q_{no.rad} \tag{1}$$

The net cooling flux is the conductive flux measured by the heat flux sensor positioned beneath the PRC sample.

The radiative heat flux emitted by the PRC sample, q_{rad}, is given by:

$$q_{rad} = \pi \int_0^\infty \bar{\varepsilon}_s(\lambda) I_b(\lambda, T_s)\, d\lambda \tag{2}$$

where $\bar{\varepsilon}_s(\lambda)$ is the angularly averaged emissivity of the PRC sample (which exhibits only weak angular dependence [31]), and $I_b(\lambda, T_s)$ is the blackbody spectral radiance at the sample temperature T_s.

The absorbed solar heat flux, q_{sol}, is:

$$q_{sol} = \alpha_{sol} G \tag{3}$$

where α_{sol} is the weighted average solar absorptivity of the PRC sample over the solar spectrum (0.3–2.5 μm), and G is the horizontal solar irradiance.

The atmospheric longwave radiation absorbed by the PRC sample, q_{atm}, is:

$$q_{atm} = \pi\, SVF \int_0^\infty \bar{\varepsilon}_s(\lambda) \varepsilon_{atm}(\lambda, RH, T_{amb}) I_b(\lambda, T_{amb})\, d\lambda. \tag{4}$$

Here, $\varepsilon_{atm}(\lambda, RH, T_{amb})$ is the spectral emissivity of the atmosphere, computed as described in Supplementary Material, Section S2. The sky view factor SVF is equal to 94 %, as calculated previously for the test site.

The thermal radiation from surrounding obstacles absorbed by the PRC sample, q_{obs}, is:

$$q_{obs} = \pi\,(1 - SVF) \int_0^\infty \bar{\varepsilon}_s(\lambda) \varepsilon_{obs}(\lambda) I_b(\lambda, T_{obs})\, d\lambda \tag{5}$$

where $\varepsilon_{obs}(\lambda)$ is the spectral emissivity of the obstacles, and $I_b(\lambda, T_{obs})$ is their blackbody spectral radiance at temperature T_{obs}. Since the obstacles consist mainly of vegetation, a constant broadband emissivity

(2.5–35 μm) of 0.95 was assumed [32], with $T_{obs} = T_{amb}$. Their contribution is weighted by the complement of the SVF, as they block part of the sky. In a typical radiative cooling performance test it is generally advisable to ensure a wide accessibility to the sky dome. The impact of any obstacle present on the horizon, however, is generally quite limited, considering that the emissivity of typical PRC materials declines steeply at large angles from the normal [31].

Finally, the term $q_{no.rad}$ accounts for non-radiative heat gains arising from convection and conduction. Owing to the thermal guarding of the sensor and the absence of significant lateral conduction paths, conductive contributions other than the measured through-thickness heat flux are neglected. Convective heat exchange is modeled as a function of wind speed via an effective heat transfer coefficient

$$q_{no.rad} = h(v)(T_{amb} - T_s), \quad (6)$$

where $h(v)$ denotes the convective heat transfer coefficient, calculated as a function of the measured wind velocity v [26]. The PRC sample temperature is estimated as $T_s = T_{ref} - R_{th}\, q_{net}$, where R_{th} is the thermal resistance of the sensor and q_{net} is defined in Eq. (1).

Given the low thermal resistance of the sensor and the strong thermal coupling to the convective heat exchanger, the resulting temperature offset ($T_{amb} - T_s$) remains sub-kelvin over the measured flux range. As a result, $q_{no.rad}$ constitutes only a second-order contribution in the model, which does not affect the overall agreement between measurements and simulations.

3. Results and discussion

3.1. Outdoor measurements

The experimental campaign was conducted for two consecutive days (6 and 7 September 2025), during which the RAFT setup, the weather station, and the infrared thermometer acquired data unattended.

Fig. 3a reports the ambient-referenced net heat flux measured by the heat-flux sensor. Owing to its optical properties, the PRC sample maintained a positive (cooling) net flux throughout the daytime, including during peak solar irradiance (approximately 830 W m^{-2}). As typically expected, cooling was more substantial during nighttime hours, with an average net flux of 64 W m^{-2} and a maximum of 85 W m^{-2}. Fig. 3b reports the air temperature measured by the weather station together with the temperature of the ambient-referenced thermal reservoir, monitored by the embedded Pt100 sensor in the aluminum interface plate. The agreement between T_{amb} and T_{ref} is within a mean absolute error (MAE) of 0.38 °C (definition in Supplementary Material, Section S3). Residual differences can be ascribed to the fact that the two sensors operate under different shielding, radiative view factors, thermal masses and ventilation conditions. Accordingly, T_{ref} is representative of the local thermal environment experienced by the RAFT assembly, whereas T_{amb} provides a standardized meteorological reference for context. Furthermore, the net heat flux is measured directly by the calibrated heat-flux sensor and is therefore independent of T_{amb}; consequently, any discrepancies between T_{ref} and T_{amb} do not propagate into the heat-flux measurement itself. Fig. 3c–d display the remaining meteorological conditions (solar irradiance, relative humidity, wind speed, and infrared sky temperature). Relative humidity was quite high during the campaign, particularly at night (59 % average RH; 69 % average nighttime RH), which limited radiative cooling performance. Wind speed was low (average 0.7 m s^{-1}). Irradiance data indicate clear-sky daytime conditions on both days. At nighttime, scattered clouds were observed during the first night between 0:00 and 3:00, as inferred from infrared sky temperature measurements showing localized temperature increases during those hours.

The RAFT setup was additionally tested over a month-long experimental campaign under varying meteorological conditions, including cloudy and fully overcast skies (Figs. S1 and S2). As shown in Supplementary Material Fig. S1, the system maintained accurate and stable net heat flux measurements together with good agreement between ambient and heat sink temperatures, confirming the effectiveness of the temperature tracking system.

3.2. Validation

The numerical model described in Section 2.4 was employed to validate the outdoor measurements obtained during the two-day campaign. The model takes as input the measured boundary conditions (ambient air temperature, relative humidity, solar irradiance, and the sample emissivity profile) and computes the net radiative cooling flux of the PRC sample, assuming that the convective heat exchanger defines an ambient-referenced thermal reservoir at $T_{ref} = T_{amb}$. The validation results are presented in Fig. 3a, where both the experimental net heat flux and the model prediction are shown.

The model reproduces the experimental trend with satisfactory accuracy, yielding a MAE of 6.6 W m^{-2} across the two experimental days. Discrepancies appear during the first three hours of the first day, resulting in a MAE of 12.5 W m^{-2} between 0:00 AM and 3:00 AM on September 6. These deviations arise from the model assumption of clear-sky conditions, whereas infrared measurements of apparent sky temperature indicate the presence of scattered clouds during those hours. The calculation of the atmospheric heat flux absorbed by the sample (q_{atm}) does not account for cloud cover. Apart from this localized deviation, the predicted downwelling atmospheric irradiance is accurate and is validated against ERA5 reanalysis data [33], as shown in Fig. S3.

In summary, the model performs reliably under clear-sky conditions and successfully validates the experimental measurements.

3.3. Discussion

The motivation for adopting a self-tracking ambient temperature setup for the outdoor characterization of PRC materials, such as RAFT, arises from the need to overcome several limitations associated with traditional indirect net heat flux measurement approaches reported in the literature [34]. A qualitative comparison between RAFT and other experimental methods used for the outdoor measurement of net cooling power of PRC materials is provided in the Supplementary Material (Table S2).

The primary advantage of RAFT lies in measuring the ambient-referenced net heat flux *directly* with a calibrated heat-flux sensor, rather than inferring it from an auxiliary energy balance. In resistive-heater approaches, the reported cooling flux is obtained from electrical power while a feedback loop uses temperature measurements to maintain $T_s \approx T_{amb}$; in calorimetric approaches, the flux is inferred from a combination of flow rate and differential temperature measurements. In both cases, the inferred cooling power can be dominated by uncertainty propagation through multiple sensors and by sensitivity to parasitic heat exchange pathways in the absence of effective thermal guarding. By contrast, RAFT reduces the inference chain to a single primary sensor, improving robustness and achieving a total heat-flux uncertainty of 1.8 W m^{-2}, which compares favorably with that achieved with state-of-the-art metrological calorimetry setups [28].

Additionally, the RAFT design does not require an accurate determination of the sample area, provided that the sample fully covers the sensitive area of the heat flux sensor. In contrast, especially with experiments involving small samples, even a small error in the determination of the exposed sample surface can represent a significant source of uncertainty in the inferred power density.

The RAFT apparatus is compact and portable, with low power consumption, as its only active component is a small fan. The system is simple to operate and achieves ambient-referenced temperature tracking without the need for an active thermal feedback controller. Additionally, it overcomes several limitations of existing net-flux measurement approaches. Unlike resistive heater-based setups, it enables measurement of both radiative cooling and heating regimes. Because heat flux is measured directly, the signal-to-noise ratio remains stable near ambient temperature, unlike temperature-difference methods. Finally, RAFT provides a local heat-flux density measurement (diameter

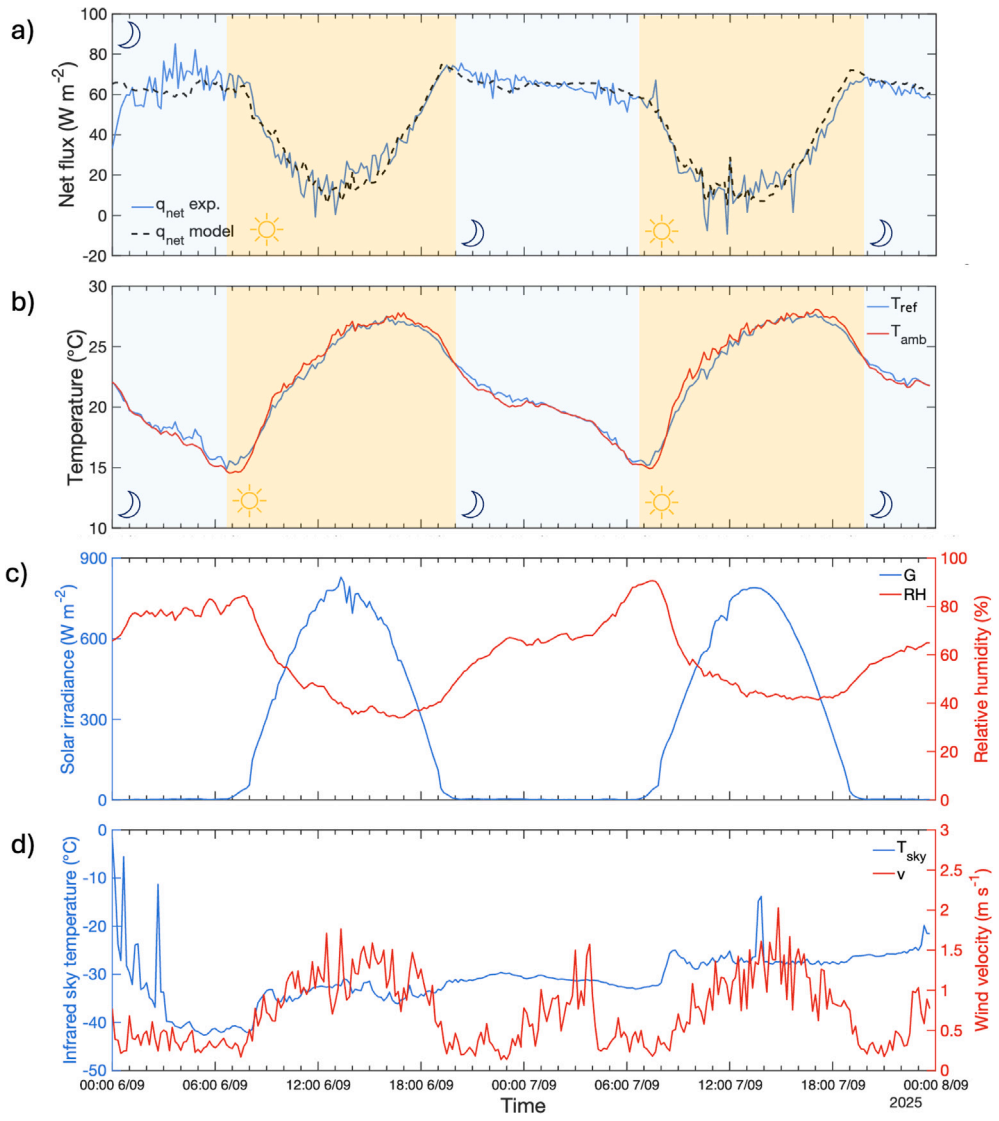

Fig. 3. Outdoor measurements (6–7 September 2025, Turin) and model validation. (a) Experimental (q_{net} exp.) and simulated (q_{net} model) PRC net flux. (b) Thermal reservoir temperature (T_{ref}) and air temperature (T_{amb}). (c) Solar irradiance (G) and relative humidity (RH). (d) Infrared sky temperature in the spectral range 8–14 μm (T_{sky}) and wind speed (v).

of the thermally guarded region: 32 mm), rather than the spatially averaged energy balance obtained with (typically much larger) liquid-flow calorimetric systems.

Outdoor experimental setups based on direct heat-flux measurements can provide reliable performance metrics for PRC materials when implemented in accordance with established best practices [9,19,20]. In particular, accurate monitoring of ambient air temperature remains essential for documenting boundary conditions and enabling meaningful comparison across experiments, as typically achieved using a professional weather station installed at the same height as the test setup. In the RAFT configuration, measurements of T_{amb} serve as a consistency check and as input for model comparison, but do not enter the computation of the net heat flux. Instead, the flux is directly referenced passively to the ambient-tracked thermal reservoir defined by the convective heat exchanger, eliminating the need to close a feedback loop on air temperature measured at a nearby but not identical location, as required by existing net-flux measurement approaches.

Additionally, the use of the infrared sky temperature sensor, despite its limited adoption in outdoor PRC studies [21,35], provides a useful diagnostic capability within the RAFT setup. It enables detection of transient cloud passages and provides a qualitative indication of the effective temperature of the sky heat sink, which helps interpret deviations between measurements and clear-sky model predictions. Extending the model to cloud- or aerosol-resolved conditions could be possible with additional atmospheric inputs, such as cloud optical properties, cloud altitude, and aerosol-related parameters [17,30,36,37] provided by ceilometers or other LIDAR instruments capable of measuring these parameters. Such developments are outside the scope of the present device-focused study, but the low-uncertainty heat-flux measurements produced by RAFT may provide useful reference data for future validation of more advanced atmospheric radiative models.

The present study is primarily focused on the direct measurement of ambient-referenced net heat-flux density, which we consider the most transferable performance metric for system integration. As such, RAFT does not aim to provide stagnation-temperature measurements within the same apparatus. While temperature-drop metrics are widely reported, they are strongly configuration-dependent (e.g., influenced by wind shielding, substrate thermal mass, non-radiative heat exchange, etc.) and may not be representative of performance when a coating is coupled to a realistic thermal load. In this sense, RAFT directly targets ambient-referenced radiative power density in a substrate-independent manner, since the radiative surface can be applied directly onto the sensor active area.

4. Conclusion

In this work, a compact device for outdoor characterization of radiative cooling materials was introduced, evaluated experimentally and validated numerically. The proposed setup, referred to as RAFT, provides an ambient-referenced approach for estimating net cooling fluxes under outdoor boundary conditions, using a convective heat exchanger.

The setup employs a heat-flux sensor for direct measurement of net heat flux, with the radiative cooling sample mounted on its sensing surface. The thermal reservoir is maintained close to local ambient temperature by a common heat sink with a low-power fan, enabling stable operation without a feedback controller. When deployed under outdoor conditions, RAFT demonstrated effective ambient temperature tracking and reliable net heat flux measurements, as confirmed by a dedicated numerical model.

The RAFT configuration addresses several limitations of conventional outdoor radiative cooling setups used for net heat flux measurements. It enables a *direct* measurement of the net heat flux, eliminating the need to infer this quantity from auxiliary measurements and thereby reducing the overall uncertainty budget to an estimated $1.8\,\mathrm{W\,m^{-2}}$. Compared with resistive heater-based systems, RAFT does not require an active feedback control, exhibits reduced measurement noise when sample temperature approaches ambient, and enables the quantification of both cooling and heating net heat fluxes. Relative to liquid-flow-based setups, RAFT offers enhanced portability, eliminates the need for fluid handling, and offers a faster response to environmental changes due to its lower thermal inertia.

Future directions could investigate whether comparable ambient tracking performance can be achieved in a fully passive configuration without forced convection, through appropriate sizing and thermal design of the heat exchanger. In addition, a metrological intercomparison between RAFT, resistive-heater-based, and liquid-flow calorimetric configurations operated side-by-side under identical meteorological conditions would enable a systematic assessment of their respective uncertainties, operational constraints, and measurement capabilities.

Overall, the experimental approach proposed in this work has the potential to become a widely adopted and low-uncertainty alternative for the outdoor evaluation of radiative cooling material heat fluxes, which is particularly significant given the current lack of rigorous and standardized experimental protocols for outdoor characterization.

Declaration of competing interest

The authors declare that they have no known competing financial interests or personal relationships that could have appeared to influence the work reported in this paper.

Acknowledgments

The authors acknowledge the project 21GRD03 PaRaMetriC, which received funding from the European Partnership on Metrology, co-financed by the European Union's Horizon Europe Research and Innovation Programme and from the Participating States; and the project FREECOOL, which received funding from the Ministero dell'Università e della Ricerca (MUR) under the frame of the Horizon Europe Cofund LEAP-SE, (GA N° 101172838).

Appendix A. Supplementary data

Supplementary material related to this article can be found online at https://doi.org/10.1016/j.applthermaleng.2026.132228.

Data availability

The experimental dataset is available in the associated Zenodo repository at https://doi.org/10.5281/zenodo.18310769. A MATLAB implementation of the numerical model used in this work is available on GitHub at https://github.com/davideforte99/Net-Heat-Flux-of-Radiative-Cooling-Materials.

References

[1] Bernard Njindan Iyke, Climate change, energy security risk and clean energy investment, Energy Econ. 129 (2024) 107225.
[2] International Energy Agency, Climate change. energy and climate are inextricably linked, 2025, https://www.iea.org/topics/climate-change. Retrieved December 21, 2025.
[3] Kaijie Yang, Xueke Wu, Lyu Zhou, Pingfan Wu, Issam Gereige, Qiaoqiang Gan, Towards practical applications of radiative cooling, Nat. Rev. Clean Technol. (2025) 1–20.
[4] Bin Zhao, Mingke Hu, Xianze Ao, Nuo Chen, Gang Pei, Radiative cooling: A review of fundamentals, materials, applications, and prospects, Appl. Energy 236 (2019) 489–513.
[5] Davide Forte, Eduardo González-Cruz, Lorenzo Pattelli, Claudio Belotti, Pietro Asinari Gloria, Matteo Fasano, Sky cooling-driven radiant-capacitive hydronic system for all-day building cooling, Appl. Energy 406 (2026) 127260.
[6] Zhen Chen, Linxiao Zhu, Wei Li, Shanhui Fan, Simultaneously and synergistically harvest energy from the sun and outer space, Joule 3 (1) (2019) 101–110.
[7] Aaswath P. Raman, Marc Abou Anoma, Linxiao Zhu, Eden Rephaeli, Shanhui Fan, Passive radiative cooling below ambient air temperature under direct sunlight, Nature 515 (7528) (2014) 540–544.
[8] Lyu Zhou, Jacob Rada, Yanpei Tian, Yu Han, Zhiping Lai, Matthew F. McCabe, Qiaoqiang Gan, Radiative cooling for energy sustainability: Materials, systems, and applications, Phys. Rev. Mater. 6 (9) (2022) 090201.
[9] Lyu Zhou, Xiaobo Yin, Qiaoqiang Gan, Best practices for radiative cooling, Nat. Sustain. 6 (9) (2023) 1030–1032.
[10] Hoang Thi Thanh Tam, Mana Toma, Takayuki Okamoto, Mio Hidaka, Kensuke Fujii, Yasuhiro Kuwana, Kotaro Kajikawa, Weatherable and solvent-soluble, paintable and transparent fluoropolymers for daytime radiative cooling, Int. J. Therm. Sci. 184 (2023) 107959.
[11] Udayan Banik, Hosni Meddeb, Dennis Berends, Nies Reininghaus, Oleg Sergeev, Luisa Busch, Kai Gehrke, Martin Vehse, Carsten Agert, Impact of parasitic heat fluxes on deep sub-ambient radiative coolers under variable pressure, Appl. Therm. Eng. 237 (2024) 121655.
[12] Huangyu Fang, Lyu Zhou, Lujia Xu, Saichao Dang, Stefaan De Wolf, Qiaoqiang Gan, Radiative cooling for vertical solar panels, Iscience 27 (2) (2024).
[13] Gimin Park, Kyeongman Roh, Hoon Kim, Salman Khan, Minjae Lee, Byung-Wook Kim, Woochul Kim, Universal experimental methods for evaluating the performance of radiative cooling materials, Adv. Mater. Technol. 7 (6) (2022) 2101205.
[14] Qimeng Song, Thomas Tran, Kai Herrmann, Tobias Lauster, Maximilian Breitenbach, Markus Retsch, A tailored indoor setup for reproducible passive daytime cooling characterization, Cell Rep. Phys. Sci. 3 (8) (2022).
[15] Ross Y.M. Wong, C.Y. Tso, Christopher Y.H. Chao, Corrected radiative cooling power measured by equivalent dissipative thermal reservoir method, Int. J. Heat Mass Transfer 174 (2021) 121341.
[16] Dongliang Zhao, Christine Elizabeth Martini, Siyu Jiang, Yaoguang Ma, Yao Zhai, Gang Tan, Xiaobo Yin, Ronggui Yang, Development of a single-phase thermosiphon for cold collection and storage of radiative cooling, Appl. Energy 205 (2017) 1260–1269.
[17] Jingyuan Huang, Chongjia Lin, Yang Li, Baoling Huang, Effects of humidity, aerosol and cloud on subambient radiative cooling, Int. J. Heat Mass Transfer 186 (2022) 122438.
[18] Zhuning Wang, Sijie Pian, Yaoguang Ma, Characterization of radiative cooling materials, Nat. Protoc. (2025) 1–39.
[19] Chenxi Sui, Po-Chun Hsu, Standardizing the thermodynamic definition of daytime subambient radiative cooling, ACS Energy Lett. 9 (6) (2024) 2997–3000.
[20] Kunlang Bu, Xingyi Huang, Xiangyu Li, Hua Bao, Consistent assessment of the cooling performance of radiative cooling materials, Adv. Funct. Mater. 33 (51) (2023) 2307191.
[21] Jérémy Werlé, Roberto Concas, Ernesto Pini, Diederik S. Wiersma, Lorenzo Pattelli, Giuseppe Emanuele Lio, Open-hardware platform for synchronous performance testing of multiple passive radiative cooling materials, Cell Rep. Phys. Sci. 6 (7) (2025).
[22] Yao Zhai, Yaoguang Ma, Sabrina N. David, Dongliang Zhao, Runnan Lou, Gang Tan, Ronggui Yang, Xiaobo Yin, Scalable-manufactured randomized glass-polymer hybrid metamaterial for daytime radiative cooling, Science 355 (6329) (2017) 1062–1066.

[23] Jyotirmoy Mandal, Yanke Fu, Adam C. Overvig, Mingxin Jia, Kerui Sun, Norman N. Shi, Hua Zhou, Xianghui Xiao, Nanfang Yu, Yuan Yang, Hierarchically porous polymer coatings for highly efficient passive daytime radiative cooling, Science 362 (6412) (2018) 315–319.
[24] Minwoo Choi, Junyong Seo, Siwon Yoon, Youngsuk Nam, Jungchul Lee, Bong Jae Lee, All-day radiative cooling using a grating-patterned PDMS, film emitter, Appl. Therm. Eng. 214 (2022) 118771.
[25] Eli A. Goldstein, Aaswath P. Raman, Shanhui Fan, Sub-ambient non-evaporative fluid cooling with the sky, Nat. Energy 2 (9) (2017) 1–7.
[26] Dongliang Zhao, Ablimit Aili, Yao Zhai, Jiatao Lu, Dillon Kidd, Gang Tan, Xiaobo Yin, Ronggui Yang, Subambient cooling of water: toward real-world applications of daytime radiative cooling, Joule 3 (1) (2019) 111–123.
[27] Ablimit Aili, Dongliang Zhao, Jiatao Lu, Yao Zhai, Xiaobo Yin, Gang Tan, Ronggui Yang, A kW-scale, 24-hour continuously operational, radiative sky cooling system: experimental demonstration and predictive modeling, Energy Convers. Manage. 186 (2019) 586–596.
[28] G. Lopardo, F. Bertiglia, G. Braccialarghe, M. Florio, F. Girard, D. Giraudi, F. Santoro, L. Pattelli, Metrological setup for accurate determination of passive radiative cooling power, Appl. Therm. Eng. (2026) 130363.
[29] A. Middel, J. Lukasczyk, R. Maciejewski, M. Demuzere, M. Roth, Sky view factor footprints for urban climate modeling, 2018.
[30] Yujie Yang, Guoqiang Zhang, Li Rong, Impact of cloud and total column water vapor on annual performance of passive daytime radiative cooler, Energy Convers. Manage. 273 (2022) 116420.
[31] A. Adibekyan, J. Schumacher, Lorenzo Pattelli, Jochen Manara, S. Meriç, Ö. Bazkir, Carlo Cucchi, C. Sprengard, G. Pérez, J. Campos, et al., Emissivity and reflectivity measurements for passive radiative cooling technologies, Int. J. Thermophys. 46 (5) (2025) 1–16.
[32] Hamlyn G. Jones, Nicole Archer, Eyal Rotenberg, Raffaele Casa, Radiation measurement for plant ecophysiology, J. Exp. Bot. 54 (384) (2003) 879–889.
[33] H. Hersbach, B. Bell, P. Berrisford, G. Biavati, A. Horányi, J. Muñoz Sabater, J. Nicolas, C. Peubey, R. Radu, I. Rozum, et al., ERA5 hourly data on pressure levels from 1940 to present, copernicus climate change service (C3S) Climate Data Store (CDS), 2023, Retrieved on December 1, 2025.
[34] Jérémy Werlé, David Tichỳ, Chrysanthi Efthymiou, Margarita-Niki Assimakopoulos, Michal Voldán, Lorenzo Pattelli, Performance assessment methods and metrics for passive daytime radiative cooling materials, Cell Rep. Phys. Sci. 7 (4) (2026).
[35] Giuseppe Emanuele Lio, Jérémy Werlé, Mariacarla Arduini, Diederik Sybolt Wiersma, Jochen Manara, Lorenzo Pattelli, Radiative cooling potential of a water-based paint formulation under realistic application conditions, ACS Appl. Opt. Mater. 2 (12) (2024) 2459–2468.
[36] Hao Chen, Jia Wei, Xiangjun Liu, Jingchong Liu, Cunhai Wang, Assessing radiative cooling power considering the cloud effects, Appl. Therm. Eng. 278 (2025) 127192.
[37] Claudio Belotti, Jochen Manara, Stephan Vidi, Lorenzo Pattelli, Jacques Hameury, Spectral longwave atmospheric irradiance determination for site- and date-specific passive radiative cooling modeling, Sustain. Energy Technol. Assessments 91 (2026) 105046.